

RESEARCH

Open Access



# Engineering a non-oxidative glycolysis pathway in *escherichia coli* for high-level citramalate production

Tingting Wang<sup>1</sup>, Lijuan Ding<sup>1,2</sup>, Huiying Luo<sup>1</sup>, Huoqing Huang<sup>1</sup>, Xiaoyun Su<sup>1</sup>, Yingguo Bai<sup>1</sup>, Tao Tu<sup>1</sup>, Yuan Wang<sup>1</sup>, Xing Qin<sup>1</sup>, Honglian Zhang<sup>1</sup>, Yaru Wang<sup>1</sup>, Bin Yao<sup>1</sup>, Jie Zhang<sup>1\*</sup> and Xiaolu Wang<sup>1\*</sup>

## Abstract

**Background** Methyl methacrylate (MMA) is a key precursor of polymethyl methacrylate, extensively used as a transparent thermoplastic in various industries. Conventional MMA production poses health and environmental risks; hence, citramalate serves as an alternative bacterial compound precursor for MMA production. The highest citramalate titer was previously achieved by *Escherichia coli* BW25113. However, studies on further improving citramalate production through metabolic engineering are limited, and phage contamination is a persistent problem in *E. coli* fermentation.

**Results** This study aimed to construct a phage-resistant *E. coli* BW25113 strain capable of producing high citramalate titers from glucose. First, promoters and heterologous *cimA* genes were screened, and an effective biosynthetic pathway for citramalate was established by overexpressing *MjcmA3.7*, a mutated *cimA* gene from *Methanococcus jannaschii*, regulated by the BBa\_J23100 promoter in *E. coli*. Subsequently, a phage-resistant *E. coli* strain was engineered by integrating the Ssp defense system into the genome and mutating key components of the phage infection cycle. Then, the strain was engineered to include the non-oxidative glycolysis pathway while removing the acetate synthesis pathway to enhance the supply of acetyl-CoA. Furthermore, glucose utilization by the strain improved, thereby increasing citramalate production. Ultimately, 110.2 g/L of citramalate was obtained after 80 h fed-batch fermentation. The citramalate yield from glucose and productivity were 0.4 g/g glucose and 1.4 g/(L·h), respectively.

**Conclusion** This is the highest reported citramalate titer and productivity in *E. coli* without the addition of expensive yeast extract and additional induction in fed-batch fermentation, emphasizing its potential for practical applications in producing citramalate and its derivatives.

**Keywords** *Escherichia coli*, Citramalate, Citramalate synthase, NOG pathway, Acetyl-CoA

\*Correspondence:

Jie Zhang  
zhangjie09@caas.cn  
Xiaolu Wang  
wangxiaolu@caas.cn

<sup>1</sup>State Key Laboratory of Animal Nutrition and Feeding, Institute of Animal Sciences, Chinese Academy of Agricultural Sciences, No.2 Yuanmingyuan West Road, Haidian district, Beijing 100193, China

<sup>2</sup>College of Animal Science, Shanxi Agricultural University, Shanxi 030600, China



© The Author(s) 2024. **Open Access** This article is licensed under a Creative Commons Attribution-NonCommercial-NoDerivatives 4.0 International License, which permits any non-commercial use, sharing, distribution and reproduction in any medium or format, as long as you give appropriate credit to the original author(s) and the source, provide a link to the Creative Commons licence, and indicate if you modified the licensed material. You do not have permission under this licence to share adapted material derived from this article or parts of it. The images or other third party material in this article are included in the article's Creative Commons licence, unless indicated otherwise in a credit line to the material. If material is not included in the article's Creative Commons licence and your intended use is not permitted by statutory regulation or exceeds the permitted use, you will need to obtain permission directly from the copyright holder. To view a copy of this licence, visit <http://creativecommons.org/licenses/by-nc-nd/4.0/>.

## Background

The extensive use of fossil fuels has caused increasing environmental pollution that has greatly threatened human health. Therefore, developing sustainable alternatives is necessary [1]. The utilization of synthetic biology and metabolic engineering has facilitated the environmentally conscious and sustainable production of various high-value products through the manipulation of microorganisms [2].

Methyl methacrylate (MMA) serves as a fundamental component in the synthesis of poly(methyl methacrylate) (PMMA), a material extensively utilized across a wide array of industries such as furniture, drug delivery systems, and the fabrication of dentures [3]. However, traditional chemical processes for MMA production rely on hazardous hydrogen cyanide and concentrated acid, leading to considerable waste generation and necessitating extensive treatment and disposal measures [4]. Recently, direct microbial production of MMA has been proposed. However, MMA is toxic to microorganisms, and no enzyme that directly catalyzes MMA formation is known [5]. Citramalate is a C5 precursor in the L-isoleucine synthesis pathway that is prevalent in various organisms [6]. It can be easily converted to methacrylic acid (MAA), an MMA precursor, through decarboxylation by alkali catalysis and dehydration in high temperature pressurized water [7]. Subsequently, MMA is produced from MAA through esterification in the presence of an acid catalyst and methanol [3]. Hence, the integration of microbial citramalate synthesis with chemical catalyst-mediated MMA conversion presents a cost-effective and environmentally friendly alternative [4].

Several metabolically engineered microorganisms capable of producing citramalate have been identified, including *Issatchenkia orientalis* [7] and *Vibrio* sp. dhg [4]. Moreover, *Escherichia coli* is a commonly used chassis in microbial cell factories owing to unique characteristics, such as a clear genetic background, high growth rates, and robustness [8]. Metabolic engineering techniques can significantly improve the ability of *E. coli* MG1655 and S17-3 to produce citramalate [6, 9]. The citramalate synthesis pathway in *E. coli* solely consists of a one-step catalytic process initiated by glycolysis precursors (pyruvate and acetyl-CoA). Hence, carbon flow via glycolysis into the acetate synthesis pathway, the tricarboxylic acid cycle (TCA), or other related pathways compete with citramalate synthesis. Consequently, efforts have been made to enhance citramalate production by attenuating these competing pathways, including the deletion of lactate and acetate pathway-related genes [10] and decreasing citrate synthase activity in the TCA cycle [6]. These strains can convert glucose into citramalate, with an output of 46.2–60.0 g/L [2, 6, 9, 11]. The highest citramalate titer previously achieved by engineered *E. coli*

BW25113 was 82.0 g/L, indicating that *E. coli* BW25113 was more suitable for citramalate production. However, studies focusing on improving citramalate titers in *E. coli* BW25113 through metabolic engineering are limited. The fed-bath fermentation process with the highest citramalate production (82.0 g/L) requires the addition of expensive yeast extract and additional induction process [12]. Additionally, phage contamination is a persistent problem in *E. coli* fermentation [13].

The supply of acetyl-coenzyme A precursor plays an important role in citramalate biosynthesis in *E. coli* [11]. Acetyl-CoA is mainly produced by decarboxylation of pyruvate whereby one carbon equivalent is lost as CO<sub>2</sub> [14]. Recently, a non-oxidative glycolysis (NOG) pathway has been proposed that can produce acetyl-CoA from glucose [15]. The NOG pathway mainly involves three steps (Fig. 1). The first step involves the conversion of fructose-6-phosphate (Fru-6P) to acetyl phosphate (AcP) and erythrose-4-phosphate (E-4P) by the phosphoketolase. Then AcP is converted to acetyl-CoA while E-4P is converted to Fru-6P by carbon rearrangements [16]. The NOG pathway has multiple advantages over the natural acetyl-CoA synthesis pathway. First, it produces acetyl-CoA from Fru-6P in two steps, which significantly reduces the complexity of multi-enzyme catalysis. Second, no CO<sub>2</sub> is released during the acetyl-CoA production, thereby maximizing carbon yield [17]. Based on this, numerous studies have enhanced the production of acetyl-CoA precursor products, such as acetone [14] and lipstatin [16], by constructing NOG pathways in microbial cell factories.

This study aimed to construct a phage-resistant *E. coli* BW25113 strain capable of producing high citramalate yields from glucose (Fig. 1). First, a citramalate-producing *E. coli* BW25113 strain with phage resistance was constructed. Second, citramalate production was improved by increasing acetyl-CoA availability and engineering glucose utilization pathways. Finally, citramalate scale production was conducted in a 10-L fermenter. This study demonstrated the potential of *E. coli* for industrial production of citramalate.

## Materials and methods

### Chemicals, strains, and growth media

Ampicillin, kanamycin, L-arabinose, and the acetyl-CoA content assay kit were procured from SolarBio (Beijing, China), while citramalate, lactate, and acetate were sourced from Sigma-Aldrich (St. Louis, MO, USA). DNA polymerase and the Gibson cloning kit were obtained from TransGen Biotech (Beijing, China). *E. coli* bacteriophage T4 (NC\_000866.4) was purchased from Zuoke Biotech (Guangzhou, China).

Table 1 shows the *E. coli* strain used in this study. *E. coli* Trans1 served for molecular cloning purposes, while

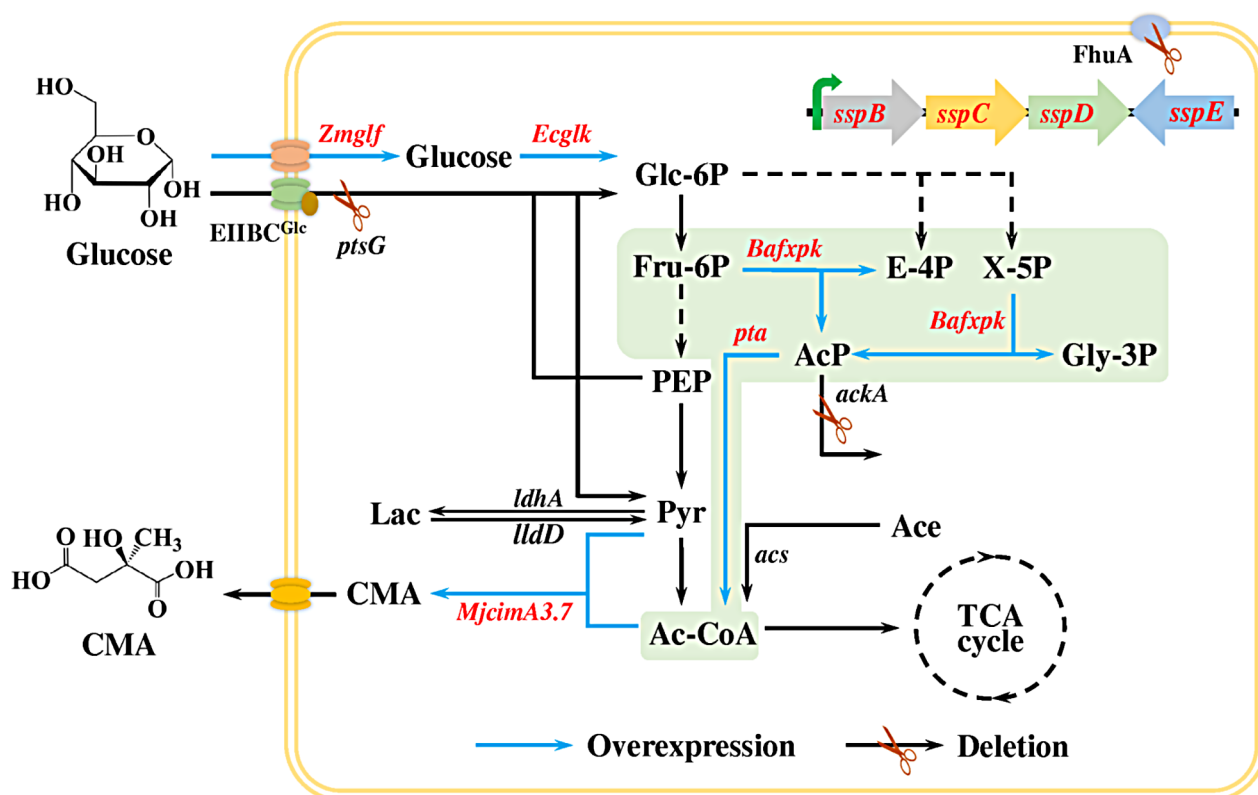


**Fig. 1** Metabolic engineering approach for citramalate biosynthesis in bacteriophage-resistant *E. coli* BW25113. Blue arrows illustrate the citramalate biosynthesis pathway. Shears indicate gene deletions, while blue arrows signify gene overexpression. TCA cycle, tricarboxylic acid cycle; Glc-6P, glucose-6-phosphate; Fru-6P, fructose-6-phosphate; E-4P, erythrose-4-phosphate; X-5P, xylulose-5-phosphate; PEP, phosphoenolpyruvate; AcP, acetyl phosphate; Gly-3P, glyceralate-3-phosphate; Lac, lactate; Pyr, pyruvate; Ace, acetate; Ac-CoA, acetyl coenzyme A; CMA, citramalate; EIIBC<sup>Glc</sup>, the glucose permease; FhuA, a ferrichrome transporter; *ptsG*, EIIBC<sup>Glc</sup> encoding gene; *Zmglf*, galactose: H<sup>+</sup> symporter encoding gene from *Zymomonas mobilis*; *glk*, glucokinase encoding gene from *E. coli*; *Bafxpk*, a bifunctional phosphoketolase encoding gene from *Bifidobacterium adolescentis*; *MjcimA3.7*, a mutated form of citramalate synthase encoding gene from *Methanococcus jannaschii*; *pta*, phosphotransacetylase encoding gene; *ldhA*, lactate dehydrogenase encoding gene; *ackA*, acetate kinase A encoding gene; *acs*, acetyl-CoA synthetase encoding gene; *lldD*, FMN-dependent lactate dehydrogenase encoding gene. The NOG pathway is highlighted with a light green background

*E. coli* BW25113 acted as the parental strain for genetic modification and citramalate production. *E. coli* strain cultivation took place in Luria-Bertani (LB) medium at 37 °C with agitation at 220 rpm in a rotary shaker. When needed, 100 mg/L ampicillin or 50 mg/L kanamycin were added to the medium.

#### Plasmids and strains construction

The plasmids and primers used in this investigation are described in Table 2 and Table S1, respectively. Plasmid construction was conducted using the Gibson assembly method.

To construct the pTarget series plasmids containing both the guide RNA (gRNA) expression cassette and repair templates, a gRNA expression cassette was amplified via polymerase chain reaction (PCR) using pRed\_Cas9\_recA as a template [18]. The resulting PCR product was cloned into pT3 vector, resulting in the desired gRNA plasmid. Subsequently, two homologous

arms (up and down arms, approximately 600 bp each) and the sequence to be inserted were separately amplified using *E. coli* BW25113 genomic DNA or synthetic DNA as templates. These fragments were then fused together via overlapping PCR to construct the donor DNA, followed by ligation to the pTarget series plasmid by Gibson assembly, which was pre-digested with *PstI/NdeI* (Fig. S1).

*HhcimA* from *Haloarchaeon* HSR6 (GenBank ID: HSR6\_1566), *MbcimA* from *Methanosarcina barkeri fusaro* (GenBank ID: Mbar\_A0217), *TtcimA* from *Tenuifilum thalassicum* (GenBank ID: FHG85\_03545), *EvcimA* from *Echinicola vietnamensis* (GenBank ID: Echvi\_2061), and *LpcimA* from *Lutibacter profundus* (GenBank ID: Lupro\_06755), *MjcimA* from *Methanococcus jannaschii* (GenBank ID: MJ1392) with 117, 132, 148, 138, 129, and 119 amino acid truncations in the C-termini, respectively, and a mutated form of *MjcimA* (*MjcimA3.7*) [12] were codon-optimized and synthesized *de novo* (BGI,

**Table 1** Strains constructed in this study

Strains	Characteristics	Sources
<b><i>E. coli</i></b>		
Trans1	<i>recA1 endA1 gyrA96 thi-1 hsdR17 supE44</i> ( $r_k^-$ , $m_k^+$ ), <i>relA1 lac</i> [ $F^+$ <i>proAB lacZ</i> ΔM15:Tn10 ( <i>tet</i> <sup>r</sup> )]	Transgen Biotech
BW25113	<i>rrnB3ΔlacZ4787 hsdR514Δ(araBAD)567Δ(rhaB AD)568 rph-1</i>	DSM 27,469
BW1	BW25113 <i>SS9::sspBCDE</i>	This study
BW2	BW1Δ <i>fhua</i> (552–558 NSEG)Δ <i>trxA</i>	This study
BW3	BW2 <i>gapC</i> site:: <i>BafxpK</i>	This study
BW4	BW3Δ <i>ackA::pta</i>	This study
BW5	BW4Δ <i>galR::ZmgIIF ΔptsG::Ecglk</i>	This study
CM0	BW25113 harboring pEASY-T3, Amp <sup>r</sup>	This study
CM1	BW25113 harboring pT3-P <sub>BAD</sub> -Mj <i>cimA</i> 3.7, Amp <sup>r</sup>	This study
CM2	BW25113 harboring pT3-P <sub>J23100</sub> -Mj <i>cimA</i> 3.7, Amp <sup>r</sup>	This study
CM3	BW25113 harboring pT3-P <sub>J23100</sub> -Hh <i>cimA</i> , Amp <sup>r</sup>	This study
CM4	BW25113 harboring pT3-P <sub>J23100</sub> -Mbc <i>imA</i> , Amp <sup>r</sup>	This study
CM5	BW25113 harboring pT3-P <sub>J23100</sub> -Tt <i>cimA</i> , Amp <sup>r</sup>	This study
CM6	BW25113 harboring pT3-P <sub>J23100</sub> -Evc <i>imA</i> , Amp <sup>r</sup>	This study
CM7	BW25113 harboring pT3-P <sub>J23100</sub> -Lpc <i>imA</i> , Amp <sup>r</sup>	This study
CM8	BW2 harboring pT3-P <sub>J23100</sub> -Mj <i>cimA</i> 3.7, Amp <sup>r</sup>	This study
CM9	BW2 harboring pT3-P <sub>J23100</sub> -Mj <i>cimA</i> , Amp <sup>r</sup>	This study
CM10	BW3 harboring pT3-P <sub>J23100</sub> -Mj <i>cimA</i> 3.7, Amp <sup>r</sup>	This study
CM11	BW4 harboring pT3-P <sub>J23100</sub> -Mj <i>cimA</i> 3.7, Amp <sup>r</sup>	This study
CM12	BW5 harboring pT3-P <sub>J23100</sub> -Mj <i>cimA</i> 3.7, Amp <sup>r</sup>	This study

Beijing, China) (Table S2). DNA fragments corresponding to *sspB*, *sspC*, *sspD*, and *sspE* were PCR-amplified using genomic DNA from *E. coli* 3234/A (GenBank ID: GCA\_001637635.1) as the template.

pT3-derived plasmids overexpressing *cimA* were constructed to identify an efficient promoter regulating critical gene overexpression. The L-arabinose-inducible promoter (P<sub>BAD</sub>) and constitutively strong promoter BBa\_J23100 (P<sub>J23100</sub>) were cloned into plasmid pEASY-T3 through TA cloning, resulting in plasmids pT3-P<sub>BAD</sub> and pT3-P<sub>J23100</sub>, respectively. Subsequently, *cimA* genes were amplified via PCR and inserted into pT3-P<sub>BAD</sub> or pT3-P<sub>J23100</sub> under the control of the respective promoter.

Gene deletion and integration were conducted utilizing the two-plasmid CRISPR-Cas9 system [19], wherein the Cas9 gene, gRNA expression cassette, and repair template were segregated into the pRed\_Cas9\_recA and pTarget series plasmids, respectively. *E. coli* BW25113 competent cells harboring pRed\_Cas9\_recA were prepared as previously described [19]. The pTarget series plasmids were introduced into respective competent cells individually through electrotransformation. L-arabinose (2.0 g/L) was used to induce the Cas9 and λ-Red recombinase expression [20]. The mutants were identified by colony PCR and sequencing. The citramalate synthesis

strain was constructed by electrotransforming the *cimA*-overexpression plasmids into the corresponding *E. coli* strains (Table 1).

### Phage infection growth curves

After culturing in LB medium overnight, a 0.1% *E. coli* seed culture was transferred into 30 mL of fresh M9 modified medium (20 g/L glucose, 5 g/L yeast extract, 15.12 g/L Na<sub>2</sub>HPO<sub>4</sub>·7H<sub>2</sub>O, 1 g/L NH<sub>4</sub>Cl, 3 g/L KH<sub>2</sub>PO<sub>4</sub>, 0.5 g/L NaCl, 11 mg/L CaCl<sub>2</sub>, 0.49 g/L MgSO<sub>4</sub>·7H<sub>2</sub>O, 1.81 mg/L MnCl<sub>2</sub>·4H<sub>2</sub>O, 2.86 mg/L H<sub>3</sub>BO<sub>3</sub>, 0.222 mg/L ZnSO<sub>4</sub>·7H<sub>2</sub>O, 0.079 mg/L CuSO<sub>4</sub>·5H<sub>2</sub>O, 0.39 mg/L Na<sub>2</sub>MoO<sub>4</sub>·2H<sub>2</sub>O, and 0.0494 mg/L Co(NO<sub>3</sub>)<sub>2</sub>·6H<sub>2</sub>O). The T4 phage was introduced into the medium when required. Cultivation was conducted in a shake incubator at 220 rpm and 37 °C, with periodic measurements of optical density at 600 nm (OD<sub>600</sub>).

### Shake-flask and fed-batch fermentation

For shake-flask fermentation, *E. coli* strains were cultured in 30 mL of LB medium supplemented with 100 mg/L ampicillin overnight. Subsequently, 0.1% seed culture was transferred into 30 mL of fresh M9 modified medium containing 100 mg/L ampicillin in 100-mL baffled shake flasks. Fermentation was conducted for 48 h in a shaker at 200 rpm at 37 °C. For strain CM1, 0.2 g/L L-arabinose was added to the culture medium to induce *Mj*cimA*3.7* expression [12]. Cultures were periodically harvested and analyzed for glucose consumption; production of citramalate, acetate, and acetyl-CoA; and OD<sub>600</sub>.

For fed-batch fermentation, cells were initially inoculated in 30 mL of LB medium in 100-mL conical flasks. Overnight cultures (0.1%) were transferred into 300 mL of LB media in 1-L conical flask as the second seed. After the second seed was cultured overnight, the contents of the shake flasks were utilized to inoculate a 10-L WMC-9010 A/S fermenter (Wanmunchun, Shanghai, China) containing 7-L fermentation medium comprising 14 g/L KH<sub>2</sub>PO<sub>4</sub>, 2 g/L Na<sub>2</sub>SO<sub>4</sub>, 4 g/L (NH<sub>4</sub>)<sub>2</sub>PO<sub>4</sub>, 1.8 g/L citric acid, and 0.6 g/L MgSO<sub>4</sub>·7H<sub>2</sub>O, supplemented with 1 mL of trace elements solution (8.4 g/L EDTA·Na<sub>2</sub>, 0.15 g/L MnCl<sub>2</sub>·4H<sub>2</sub>O, 2.5 g/L CoCl<sub>2</sub>·2H<sub>2</sub>O, 1.5 g/L CuCl<sub>2</sub>·2H<sub>2</sub>O, 2.5 g/L Na<sub>2</sub>MoO<sub>4</sub>·2H<sub>2</sub>O, 3 g/L H<sub>3</sub>BO<sub>3</sub>, 13 g/L Zn(CH<sub>3</sub>COO)<sub>2</sub>·2H<sub>2</sub>O, and 10 g/L ferric citrate), 20 g/L glucose, and 100 mg/L ampicillin. To uphold the relative concentration of dissolved oxygen, the fermentation was conducted at 37 °C with agitation at 800 rpm [21]. NH<sub>4</sub>OH was used to stabilize the pH of the fermentation solution at 7.0. Once the initial glucose was depleted, a fed-batch medium containing 2 g/L MgSO<sub>4</sub>·7H<sub>2</sub>O, 700 g/L glucose, and 1 mL trace elements solution was introduced into the fermentation broth, with the glucose concentration maintained below 10 g/L.

**Table 2** Plasmids used in this study

Plasmid	Characteristics	Sources
pRed_Cas9_recA	Temperature-sensitive plasmid, including oriR101, repA101, $\lambda$ -Red recombinase, and Cas9 controlled by an L-arabinose-inducible promoter ( $P_{BAD}$ ), Kan <sup>r</sup>	[18]
pEASY-T3	pUC origin, f1 origin, <i>Lac</i> operator, Amp <sup>r</sup>	Transgen Biotech
pTarget-sspB	Derived from pEASY-T3 for the insertion of <i>sspB</i> from <i>E. coli</i> 3234/A at the SS9 site	This study
pTarget-sspC	Derived from pEASY-T3 for the insertion of <i>sspC</i> from <i>E. coli</i> 3234/A at the SS9 site	This study
pTarget-sspD	Derived from pEASY-T3 for the insertion of <i>sspD</i> from <i>E. coli</i> 3234/A at the SS9 site	This study
pTarget-sspE	Derived from pEASY-T3 for the insertion of <i>sspE</i> from <i>E. coli</i> 3234/A at the SS9 site	This study
pTarget- $\Delta$ fhuA(552–558 NSEG)	Derived from pEASY-T3 for FhuA (552–558 NSEG) deletion	This study
pTarget- $\Delta$ trxA	Derived from pEASY-T3 for <i>trxA</i> deletion	This study
pTarget-fxpk	Derived from pEASY-T3 for the insertion of the $P_{J23102}$ - <i>Bafxpk</i> cassette at the gapC site	This study
pTarget- $\Delta$ ackA::pta	Derived from pEASY-T3 for the <i>ackA</i> knockout and the $P_{trc}$ - <i>pta</i> cassette knockin	This study
pTarget- $\Delta$ galR::glf	Derived from pEASY-T3 for the <i>galR</i> knockout and the $P_{m12}$ - <i>ZmgIf</i> cassette knockin	This study
pTarget- $\Delta$ ptsG::glk	Derived from pEASY-T3 for the <i>ptsG</i> knockout and the $P_{m12}$ - <i>Ecglk</i> cassette knockin	This study
pT3- $P_{BAD}$	Derived from pEASY-T3 with $P_{BAD}$ integrated into the MCS	This study
pT3- $P_{BAD}$ -MjcmA3.7	T3- $P_{BAD}$ containing <i>MjcmA3.7</i> gene under the control of $P_{BAD}$ promoter	This study
pT3- $P_{J23100}$	Derived from pEASY-T3 containing the $P_{J23100}$ in the MCS	This study
pT3- $P_{J23100}$ -MjcmA3.7	T3- $P_{J23100}$ containing the <i>MjcmA3.7</i> gene under the control of $P_{J23100}$	This study
pT3- $P_{J23100}$ -HhcmA	T3- $P_{J23100}$ containing the truncated <i>HhcmA</i> gene under the control of $P_{J23100}$	This study
pT3- $P_{J23100}$ -MbcimA	T3- $P_{J23100}$ containing the truncated <i>MbcimA</i> gene under the control of $P_{J23100}$	This study
pT3- $P_{J23100}$ -TtcimA	T3- $P_{J23100}$ containing the truncated <i>TtcimA</i> gene under the control of $P_{J23100}$	This study
pT3- $P_{J23100}$ -EvcimA	T3- $P_{J23100}$ containing the truncated <i>EvcimA</i> gene under the control of $P_{J23100}$	This study
pT3- $P_{J23100}$ -LpcimA	T3- $P_{J23100}$ containing the truncated <i>LpcimA</i> gene under the control of $P_{J23100}$	This study
pT3- $P_{J23100}$ -MjcmA	T3- $P_{J23100}$ containing the <i>MjcmA</i> gene under the control of $P_{J23100}$	This study

### Analytical methods

Cell growth was determined by measuring the OD<sub>600</sub> using a spectrophotometer (BioTek, Winooski, Vermont, USA). A 1-L cell suspension with an OD<sub>600</sub> of 1, obtained through fermentation in M9 modified medium, was centrifuged at 12,000 × *g* for 5 min at 4 °C, and the sample was washed three times with water. After the supernatant was removed, the samples were dried at 80 °C for 24 h [22]. The dry cell weight (DCW) of *E. coli* was evaluated by the DCW/OD<sub>600</sub>-correlation (0.4 g/L/OD<sub>600</sub>).

Cell-free extracts of CM0–7 were prepared from cultures grown in M9 modified medium for 48 h. L-arabinose was added to a final concentration of 0.2 g/L for induction when needed. Cells were harvested by centrifugation (12,000 × *g*, 20 min, 4°C) and resuspended in 50 mM Na<sub>2</sub>HPO<sub>4</sub>-NaH<sub>2</sub>PO<sub>4</sub> buffer (pH 7.5) containing 500 mM NaCl. After the cells were lysed by ultrasound, the cell debris were removed by centrifugation at 12,000 × *g* for 20 min at 4°C. For the citramalate synthase assay, the soluble extract was dissolved in 100  $\mu$ L of 0.1 M TES buffer (pH 7.5) containing 1 mM of acetyl-CoA and 1 mM of pyruvate. After incubation at 37°C for 1 h, 50  $\mu$ L of 10 mM 5,5'-dithio-bis(2-nitrobenzoic acid) in 0.1 M Tris-HCl (pH 8.0), 70  $\mu$ L of 1 M Tris-HCl (pH 8.0), and 780  $\mu$ L of ddH<sub>2</sub>O were added to the solution. The OD<sub>412</sub> was recorded. A standard curve was used to calculate the CoASH concentrations [23]. CimA activity of one unit (U) is defined as the catalytic synthesis of 1

$\mu$ mol of CoA per minute at 37 °C [12]. The specific activity was denoted as U/g DCW cells. For the analysis using sodium dodecyl sulfate polyacrylamide gel electrophoresis (SDS-PAGE), the soluble extract was mixed with 5 × SDS-PAGE loading buffer, boiled for 5 min, and equivalent volumes of the samples were loaded onto the gels [24]. Acetyl-CoA concentration was determined as previously described [21].

Glucose, citramalate, lactate, and acetate concentrations were determined utilizing a high performance liquid chromatography (HPLC) system (Shimadzu, Kyoto, Japan) outfitted with a refractive index detector (RID-20 A; Shimadzu, Kyoto, Japan), employing an Aminex® HPX-87 H Column (300×7.8 mm, Bio-Rad, Hercules, CA, USA) at 35 °C with 5 mM H<sub>2</sub>SO<sub>4</sub> (0.5 mL/min) serving as the mobile phase [12].

### Phylogenetic analysis

The six CimA amino acid sequences were aligned via the ClustalW algorithm in MEGA-X, followed by constructing a phylogenetic tree using the neighbor-joining method. Bootstrap analysis was performed to assess the reliability of the trees, with the parameter set to 1000. Default values were applied for the other parameters.

### Statistical analysis

The Statistical Package for the Social Sciences (SPSS) software (Version 19.0, IBM, Armonk, NY, USA) was

used to analyze the data via one-way analysis of variance (ANOVA).

## Results

### Citramalate synthesis pathway construction

Citramalate can be synthesized by expressing heterogenous citramalate synthase encoded by *cimA* in *E. coli* BW25113 [12]. To screen an efficiency promoter that regulates key gene overexpression, strains CM1 and CM2 harboring pT3-PBAD-MjcmA3.7 and pT3-P<sub>J23100</sub>-MjcmA3.7 (Fig. 2A and S2), respectively, were constructed, wherein *MjcmA3.7* was expressed, driven by an inducible promoter (P<sub>BAD</sub>) and a strongly constitutive promoter (P<sub>J23100</sub>), respectively (Table 1). Citramalate production was performed by shake-flask fermentation.

For CM1, *MjCimA3.7* overexpressing was induced by 0.2 g/L L-arabinose [12]. Glucose consumption, OD<sub>600</sub>, and citramalate titers in the medium were almost stagnant after 26 h of fermentation (Fig. 2B). Both CM1 and CM2 exhibited similar glucose consumption and growth profiles: 9.2 and 8.7 g/L glucose was consumed by strains CM1 and CM2, respectively, and the maximum OD<sub>600</sub> was 2.0 and 2.2, respectively, after 48 h of fermentation. However, citramalate production was significantly different. The citramalate titer of CM2 was 3.8 g/L, which was 6.3-fold higher than that in CM1 (0.6 g/L) (Fig. 2B). In line with the preceding findings, the CimA activity of the CM2 cell-free extract measured 4.1 U/g DCW, signifying a 3.4-fold increase compared to that of CM1 (1.2 U/g DCW) (Fig. S3). Thus, the use of a constitutive promoter

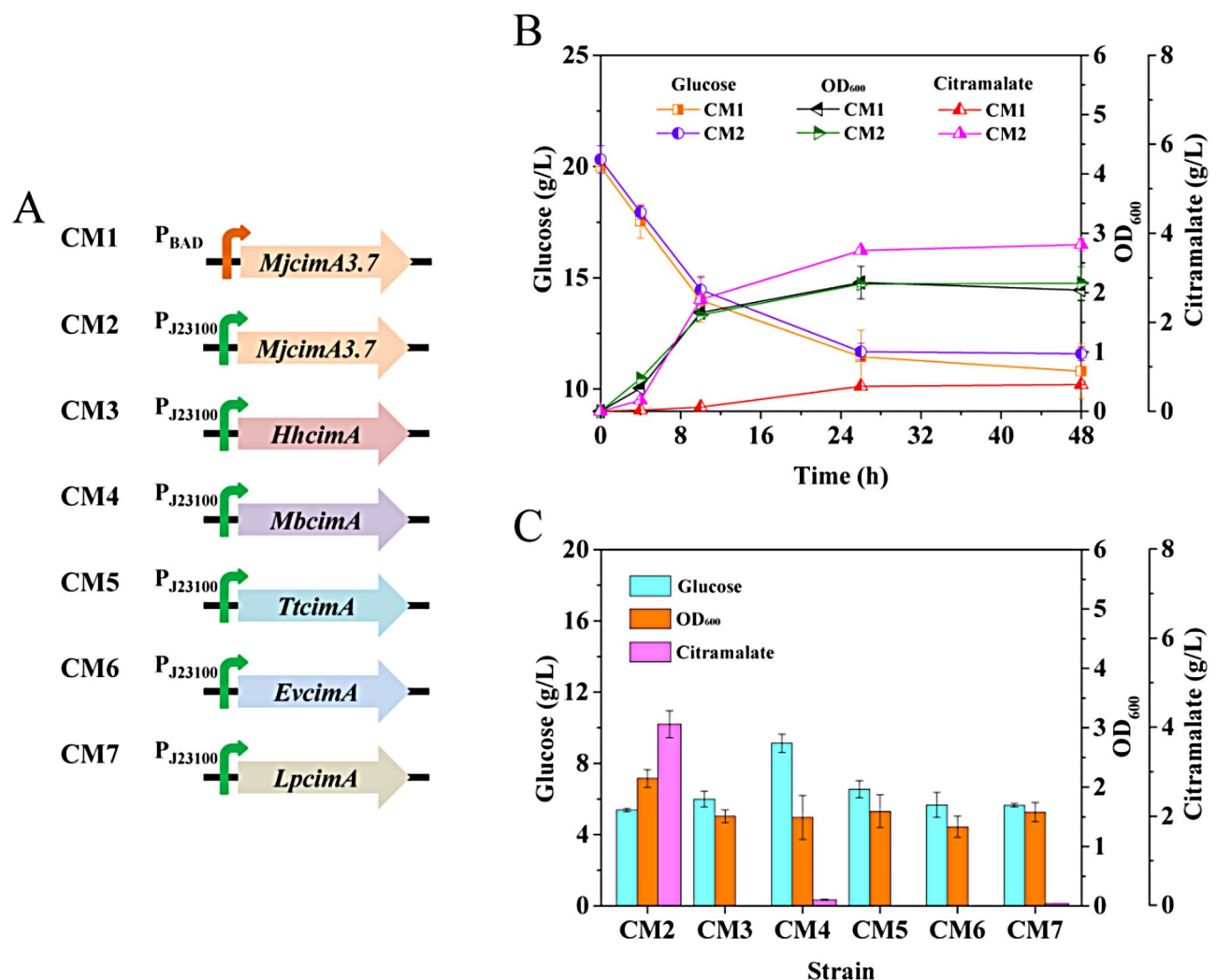


**Fig. 2** Construction of the citramalate biosynthesis pathway in *E. coli* BW25113. **(A)** A schematic diagram of the expression cassettes utilized for the strains. **(B)** Screening of promoters suitable for expressing CimA in *E. coli* BW25113. **(C)** Screening of CimA variants suitable for catalyzing the biosynthesis of citramalate in *E. coli* BW25113. Strains were cultured in 30 mL of M9 modified medium at 37 °C for 48 h with agitation at 220 rpm in a rotary shaker. L-arabinose was added to the culture medium at a concentration of 0.2 g/L when necessary. Glucose consumption, OD<sub>600</sub>, and citramalate production were measured periodically

( $P_{J23100}$ ) in *E. coli* BW25113 for *cimA* expression was more efficient for citramalate production using glucose as a carbon source.

Moreover, an efficient CimA must be selected to efficiently produce citramalate in *E. coli* [7]. Hence, new *cimA* genes were searched in the NCBI database, and phylogenetic analysis was performed. Five genes (*HhcimA*, *MbcimA*, *TtcimA*, *EvcimA*, and *LpcimA*) were selected that were highly diverse in the phylogenetic tree (Fig. S4). To eliminate feedback inhibition by L-isoleucine, the L-isoleucine-binding domain coding regions of *cimA* genes were deleted [23] and cloned into pT3- $P_{J23100}$  (Table 2). These five plasmids were introduced into *E. coli* BW25113 through transformation, generating strains CM3–7 (Table 1; Fig. 1A). Shake flask fermentation was performed for 48 h, and CM2 was used as the control. Cells were harvested and SDS-PAGE analysis was conducted. Additional protein bands were observed at approximately 45 kDa in strains CM2, CM3, CM4, CM6, and CM7 compared with that of the CM0 strain with the pEASY-T3 plasmid (Table 1 and Fig. S5). This result indicated that all *cimA* genes (except *TtcimA*) were expressed in *E. coli*. As shown in Fig. 2C, glucose consumption and the  $OD_{600}$  of CM2 were 5.4 g/L and 2.1, respectively, with a citramalate titer of 4.1 g/L. While strain CM4 exhibited higher glucose consumption (9.1 g/L) compared to CM2, both the  $OD_{600}$  and citramalate titer (1.5 and 0.1 g/L, respectively) were notably lower than those of CM2. The glucose consumption and  $OD_{600}$  of CM3, CM5, CM6, and CM7 were similar, whereas citramalate was only produced by CM7 (0.04 g/L) (Fig. 2C), suggesting that *HhcimA*, *TtcimA*, and *EvcimA* were unsuitable for citramalate production in *E. coli* BW25113. Overall, these

investigations indicated that no *cimA* variants caused higher citramalate production in *E. coli* BW25113 than that caused by *MjCimA3.7*. Thus, a citramalate synthesis pathway was constructed in strain CM2 by overexpressing *MjCimA3.7* under the control of  $P_{J23100}$ .

### Construction of bacteriophage-resistant citramalate-producing strain

A citramalate biosynthesis pathway was successfully constructed in *E. coli* BW25113. However, phage outbreaks can cause severe disruptions in industrial fermentation processes, leading to substantial financial losses. By inserting the *sspBCDE* gene cassette from *E. coli* 3234/A into the genome of the strain, together with mutating *fhuA*, a ferrichrome transporter found in the outer membrane, and deleting *trxA*, a processivity factor associated with T7 DNA polymerase for phage DNA synthesis produced highly phage-resistant *E. coli* MG1655 and W3110 strains. These strains exhibit resilience against a diverse spectrum of phages while maintaining genomic and fermentation stability [25]. To generate the phage-resistant strain, the *sspBCDE* gene cassette was integrated into safe site 9 (SS9) of the BW25113 chromosome in segments using the CRISPR-Cas9 system to generate the BW1 strain [26]. Strain BW2 was constructed by deleting *trxA* and extracellular loop 8 (552–558 NSEG) of FhuA in BW1 (Table 1) [25]. The engineered strain BW2's resistance to bacteriophages was examined in M9 modified medium. To avoid serious laboratory phage contamination, only the common T4 phage found in the laboratory and factory was used [27]. As shown in Fig. 3A, T4 phage contamination significantly inhibited *E. coli* BW25113 growth. This engineering strategy slightly inhibited cell

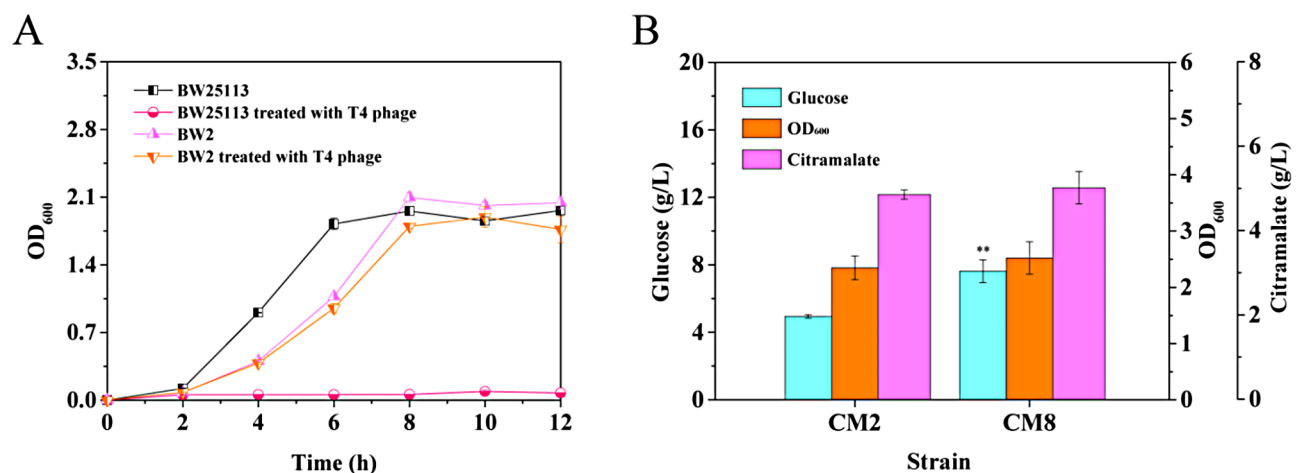


**Fig. 3** Citramalate production performance of the strain with the SspBCDE defense system. **(A)** The resistance of the strain to T4 phage. Strains were inoculated in 30 mL of M9 modified medium at 37 °C for 48 h with agitation at 220 rpm in a rotary shaker. T4 phage was introduced into the culture medium when necessary, and  $OD_{600}$  was periodically monitored. **(B)** Comparison of citramalate synthesis between strain CM2 without T4 phage and phage-resistant strain CM8 in the presence of T4 phage. Strains were inoculated in 30 mL of M9 modified medium at 37 °C for 48 h with agitation at 220 rpm in a rotary shaker. Glucose consumption,  $OD_{600}$ , and citramalate production were measured periodically. Asterisks denote significance compared to CM2: \*\* indicates  $p < 0.01$ , one-way ANOVA test

growth, similar to previous reports [25]. The  $OD_{600}$  of BW2 was 0.4 after 4 h of cultivation, reaching 2.1 after 8 h without T4 phage (Fig. 3A). BW2 exhibited resistance to the T4 phage and demonstrated growth profiles akin to those of BW2 devoid of phage infection. When treated with the T4 phage, the  $OD_{600}$  of BW2 reached 1.8 after 8 h of cultivation, comparable to wild-type *E. coli* BW25113 without T4 phage (2.0) (Fig. 3A). Therefore, the aforementioned strategy is suitable for constructing the phage-resistant *E. coli* BW25113 strain.

Subsequently, the phage-resistant strain was assessed for citramalate production while conferring protection against phage infections. The pT3-P<sub>J23100</sub>-MjCimA3.7 was transformed into BW2, generating CM8 (Table 1), and citramalate production was examined by shake-flask fermentation in the presence of the T4 phage. CM2 uninfected with the phage was used as the control. Following 48 h of cultivation, CM8 exhibited glucose consumption of 7.6 g/L, marking a 55.1% increase compared to that of CM2 (4.9 g/L) (Fig. 3B). The  $OD_{600}$  of CM8 was

2.5, comparable with that of CM2 (2.3). While showing strong tolerance to T4 phage, CM8 also produced 5.0 g/L citramalate, which was comparable with that of CM2 without phage challenge (4.9 g/L), indicating that the citramalate production of the phage-resistant strain was not significantly affected. Therefore, the phage-resistant citramalate-producing strain CM8 was selected for subsequent studies.

#### Improving acetyl-CoA supply by introducing the non-oxidative glycolysis (NOG) pathway

Compared with *E. coli* expressing the wild-type MjCimA, the strain expressing the mutant MjCimA3.7 has a higher 1-propanol yield, which utilizes citramalate as a precursor [23]. Hence, the citramalate synthesis capacity of these two CimAs was confirmed. CM9 was constructed by transforming pT3-P<sub>J23100</sub>-MjCimA into BW2, and the citramalate production capacities of CM8 and CM9 were characterized. As depicted in Fig. 4A and B, the CM8 strain produced 4.0 g/L of citramalate, yielding

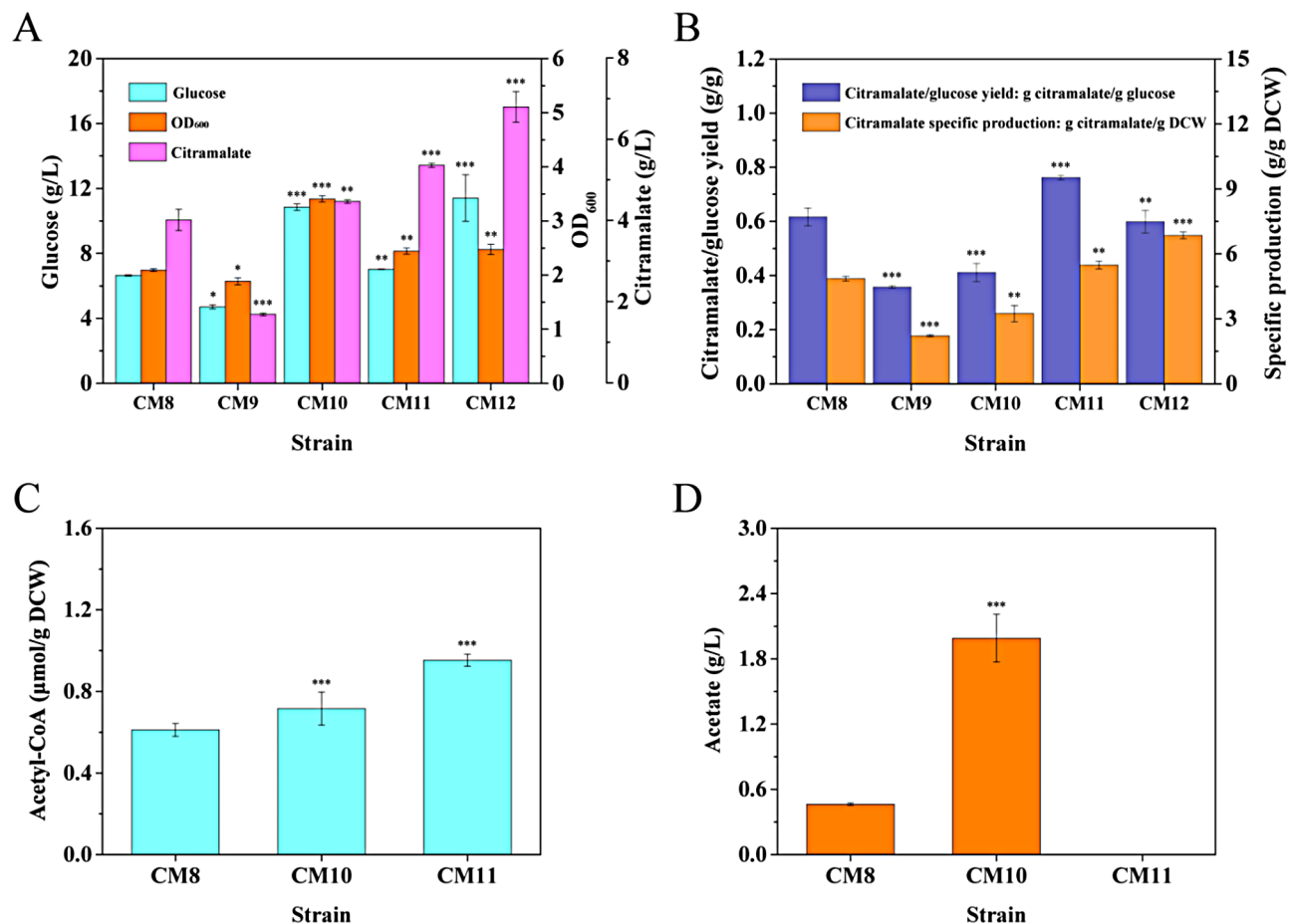


**Fig. 4** Citramalate production performance of engineered strains. Strains were inoculated in 30 mL of M9 modified medium at 37 °C for 48 h with agitation at 220 rpm in a rotary shaker. Glucose consumption,  $OD_{600}$ , and citramalate production of strains (A), citramalate yield on glucose and specific production (B), intracellular acetyl-CoA (C), and acetate concentrations (D) were quantified. Asterisks indicate significance compared to CM8: \*\*\* indicates  $p < 0.001$ , \*\* indicates  $p < 0.01$ , \* indicates  $p < 0.05$ , one-way ANOVA test

0.6 g/g glucose and 4.9 g/g DCW, which were 2.4-, 1.5-, and 2.2-fold higher than those of CM9 (1.7 g/L, 0.4 g/g glucose, and 2.2 g/g DCW, respectively). The g/g DCW is an important parameter that reflects the efficiency of microbial production of the target product and serves as a standardized indicator that can effectively compare the genetic modification strategies [28, 29].

These results confirmed that *MjCimA3.7* was more beneficial for citramalate production in *E. coli* BW25113 than wild-type *MjCimA*. The  $k_{cat}$  and  $K_m$  values for acetyl-CoA of *MjCimA3.7* were enhanced approximately 3.0-fold compared to the wild-type level [23]. Therefore, the acetyl-CoA supply may be a bottleneck for citramalate synthesis in *E. coli* BW25113. Based on these findings, the NOG pathway was introduced into the citramalate-producing strain [14]. A bifunctional phosphoketolase gene (*Bafxpk*) from *Bifidobacterium adolescentis* under the control of  $P_{J23102}$  was inserted into the gapC site of strain BW2, resulting in the BW3 [30]. The pT3- $P_{J23100}$ -*MjCimA3.7* was transformed into BW3, generating CM10. As shown in Fig. 4A, CM10 showed obvious increases in glucose consumption and OD<sub>600</sub> (10.9 g/L and 3.4, respectively) compared with that of CM8, which was consistent with a previous study [17]. CM10 exhibited citramalate production of 4.5 g/L, which is a 12.5% increase compared to CM8. The acetyl-CoA concentrations in strain CM10 were 16.7% higher than that in strain CM8 (0.7 and 0.6  $\mu$ mol/g DCW, respectively) (Fig. 4C). This result showed that the enhanced supply of acetyl-CoA precursor by integrating the NOG pathway into *E. coli* could significantly increase the citramalate yield [11]. However, the citramalate yield on glucose and specific production obtained using CM10 were 0.4 g/g glucose and 3.2 g/g DCW, respectively, which were 33.3% and 34.7% lower than those of CM8 (Fig. 4B). Following phosphoketolase activity, the resultant product, acetyl phosphate, can be catalyzed by phosphotransacetylase to produce acetyl-coA, and can also be catalyzed by acetate kinase A to produce acetate. The phosphotransacetylase and acetate kinase A were encoded by *pta* and *ackA*, respectively [31]. The acetate titer increased to 2.0 g/L as a by-product in CM10, which was 4.0-fold higher than that of CM8 (0.5 g/L), indicating a significant metabolic flux overflow toward acetate [14]. This also explains the low citramalate yield on glucose and specific production of CM10 compared with those of CM8 (Fig. 4B).

To further direct the metabolic flux to acetyl-CoA, *ackA* was replaced with the  $P_{trc}$ -*pta* cassette on the BW3 chromosome [30], resulting in the BW4 strain. The pT3- $P_{J23100}$ -*MjCimA3.7* was transformed into BW4, generating CM11, and citramalate production by CM11 was performed. As shown in Fig. 4A, the glucose consumption and OD<sub>600</sub> of CM11 were 7.0 g/L and 2.4, respectively, during shake-flask fermentation. The intracellular

concentration of acetyl-CoA rose by 42.9% compared to that in CM10 (Fig. 4C). Moreover, acetate was undetected in the CM11 strain (Fig. 4D). The citramalate production, citramalate yield on glucose, and citramalate specific production by this strain were further increased to 5.4 g/L, 0.8 g/g glucose, and 5.5 g/g DCW, respectively, which is 35.0%, 33.3%, and 12.2% higher than those obtained in CM8, respectively (Fig. 4A and B). These results imply that *ackA* deletion and *pta* overexpression channel acetyl phosphate to form acetyl-CoA, consequently favoring citramalate production.

### Increased glucose utilization to increase citramalate production

An unfavorable trait of the CM11 strain was its reduced glucose consumption, which marked a 35.8% decrease compared to that of CM10 during shake-flask fermentation. We hypothesized that enhancing the glucose uptake capacity could induce improved production properties in the CM11 strain [32]. In *E. coli*, glucose uptake and phosphorylation are mediated by the phosphoenolpyruvate (PEP): carbohydrate phosphotransferase system (PTS), and one phosphoenolpyruvate is consumed to produce one pyruvate in this process [33]. Based on a prior investigation aiming to enhance glucose utilization and consequently elevate the acetyl-CoA supply in *E. coli* [32], BW5 underwent modification by substituting native *ptsG* and *galR*, responsible for encoding a membrane component of the glucose-specific PTS and a galactose repressor, respectively, with *EcgIk* (encoding *E. coli* glucokinase) and *ZmgIf* (encoding galactose: H<sup>+</sup> symporter from *Zymomonas mobilis*), correspondingly, controlled by  $P_{m12}$ . The resulting host BW5 was transformed with the pT3- $P_{J23100}$ -*MjCimA3.7* plasmid, generating CM12. As a result, CM12 had a 62.9% increase in glucose consumption of 11.4 g/L under shake-flask fermentation, compared with that of CM11. Moreover, CM12 exhibited a similar growth profile compared with that of CM11 (Fig. 4A). Despite CM12 exhibiting a citramalate yield of 0.6 g/g glucose, which was 25.0% lower than that of CM11 and comparable to that of CM8, its citramalate titer and citramalate specific production increased to 6.8 g/L and 6.9 g/g DCW, respectively, which were both 1.3-fold higher than those of CM11, respectively (Fig. 4A and B).

### Fed-batch production of citramalate in a 10-L fermenter

To further assess the impact of metabolic engineering strategies on citramalate production, fed-batch fermentations of CM8, CM11, and CM12 were conducted in 10-L fermenters. As depicted in Fig. 5, the initial glucose (20 g/L) was exhausted after approximately 16 h of fermentation. The fed-batch medium was added to the fermentation broth, and the glucose concentration was

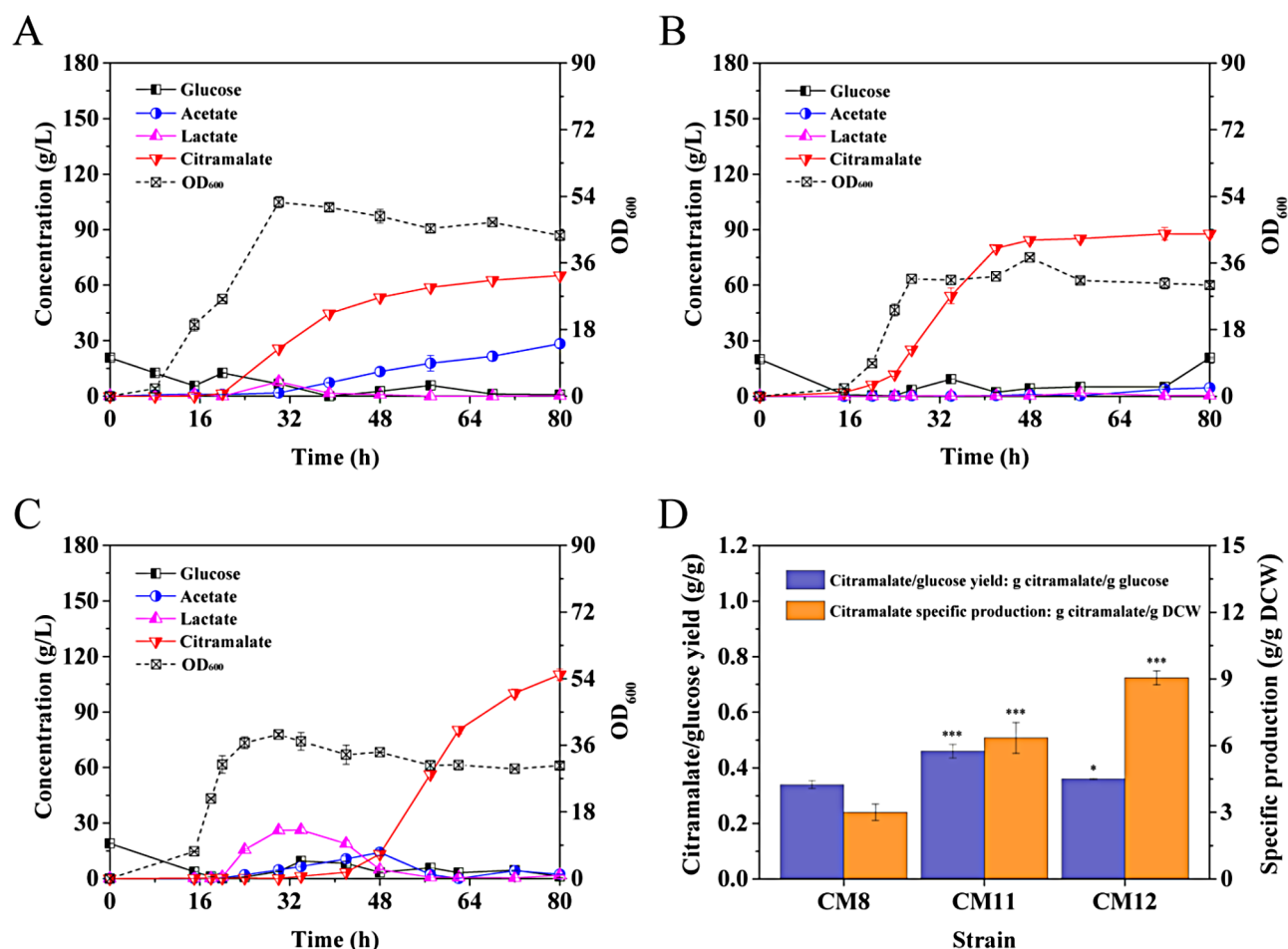


**Fig. 5** Fed-batch fermentation profiles of engineered strains. *E. coli* strains were cultured in 10-L fermenters containing 7-L of fermentation medium for 80 h, and samples were periodically collected. Concentrations of glucose, acetate, lactate, and citramalate, as well as OD<sub>600</sub> of CM8 (A), CM11 (B), CM12 (C), and citramalate yield on glucose and specific production (D) were quantified. Asterisks indicate significance compared to CM8: \*\*\* indicates  $p < 0.001$ , \*\* indicates  $p < 0.01$ , One-Way ANOVA test

maintained at <10 g/L. CM8 attained a higher OD<sub>600</sub> (52.4) compared to those of CM11 and CM12 (37.5 and 38.9, respectively), but exhibited significantly lower citramalate production (65.2 g/L) (Fig. 5A–C). This may also be owing to the accumulation of the acetate byproduct in CM8, which was 28.4 g/L after 80 h of fermentation (Fig. 5A). Consistent with the results of the shake-flask fermentations, the final production titer of citramalate in CM11 was significantly increased to 87.7 g/L, 1.3-fold higher than that produced by CM8 (Fig. 5A and B); moreover, the citramalate yield on glucose and specific production by CM11 increased to 0.5 g/g glucose and 6.4 g/g DCW, respectively, marking a 1.7- and 2.1-fold increase compared to those by CM8 (0.3 g/g glucose and 3.0 g/g DCW, respectively) (Fig. 5D). These results further supported that implementing the NOG pathway in *E. coli* BW25113 enhanced the production and yield of citramalate by increasing the acetyl-CoA supply. The yield of citramalate from glucose was lower in the fermenter than

**Table 3** Overviews of citramalate production by *E. Coli* strains

Strains	Titre (g/L)	Yield (g/g glucose)	Productivity (g/(L-h))	Period (h)	Reference
MG1655	46.5	0.8	0.4	132	[11]
MG1655	54.1	0.6	0.6	87	[2]
BW25113	82.0	0.5	1.3	65	[10]
MG1655	60.0	0.5	0.4	132	[6]
S17-3	46.2	0.8	0.6	72	[9]
BW25113	110.2	0.4	1.4	80	This study

that in the shaking flask. A possible explanation for this is that more acetyl-CoA is consumed by the TCA cycle [11, 32].

The citramalate titer of the final strain CM12 was 110.2 g/L after 80 h fermentation (Fig. 5C; Table 3), which was 25.7% higher than that of CM11. While the fermentation was stopped after 80 h for consistency with previous results, extending the fermentation duration could potentially yield higher citramalate titers. Additionally, the citramalate yield on glucose was 0.4 g/g glucose,

20.0% lower than CM11 but similar to CM8, while the citramalate specific production was 9.1 g/g DCW, 42.2% higher than CM11 (Fig. 5D). This was consistent with the results of the shake-flask fermentation. Unlike CM8 and CM11, citramalate production by CM12 showed a lag phase, and lactate was produced before citramalate synthesis (Fig. 5A–C). The concentrations of the common by-products lactate and acetate in the fermentation broth were highest after 34 and 48 h, reaching 26.2 and 14.1 g/L, respectively. In *E. coli*, acetate can be catalyzed to acetyl-CoA by acetyl-CoA synthase and lactate can be reutilized by flavin mononucleotide-dependent lactate dehydrogenase [34, 35]. These by-products were re-assimilated during fermentation to provide a source for pyruvate and citramalate presumably, leaving only 1.8 g/L lactate and 2.3 g/L acetate at the end of fermentation (Fig. 5C).

In summary, high citramalate production was achieved in fed-bath fermentation by CM12 with multistep metabolic engineering. To our knowledge, the citramalate production of 110.2 g/L and productivity of 1.4 g/(L·h) reported in this study represent the highest levels achieved using *E. coli*, without the addition of costly yeast extract and L-arabinose to the fed-batch medium (Table 3).

## Discussion

Metabolic engineering is a powerful tool for regulating the metabolic pathways of microorganisms towards the production of desired compounds from low-cost glucose [24]. Citramalate is a chemical precursor of PMMA with diverse industrial applications [9]. To date, *E. coli* BW25113 is the most efficient host for citramalate biosynthesis using glucose as the carbon source [12]. However, further research is necessary to improve citramalate production and eliminate the dependence of yeast extract and induction process in fed-bath fermentation process [12]. Additionally, phage contamination is a persistent problem during fermentation [13]. In this study, optimization strategies aimed at enhancing citramalate production in the bacteriophage-resistant *E. coli* BW25113 strain were explored.

Functional CimA expression is a key step in *E. coli* citramalate biosynthesis [7]. In this study, the use of a strongly constitutive promoter ( $P_{J23100}$ ) to drive *cimA* expression was found to be more beneficial than the  $P_{BAD}$  used previously for citramalate production in *E. coli* using glucose as a carbon source. This may be because the transcriptional activity of  $P_{BAD}$  is inhibited by the presence of glucose [36]. Evaluation of CimAs for citramalate biosynthesis in *E. coli* has been limited to only a few instances [2, 9, 11]. As protein sequence databases rapidly expand, a more efficient natural CimA has been identified. Two *cimA* genes from *Methanosarcina*

*barkeri* Fusaro (*MbcimA*) and *Lutibacter profundus* (*LpcimA*) other than *MjcimA3.7* were active in *E. coli* and were verified for the first time. However, no CimA variants yielding higher citramalate than *MjCimA3.7* were found. High sequence diversity was observed among CimA sequences, with only 28.6–53.1% identities at the protein level (Fig. S6), and no clear sequence-function relationships were evident [7]. Thus, a citramalate biosynthesis pathway was constructed in *E. coli* BW25113 by *MjcimA3.7* overexpression under the control of  $P_{J23100}$ . In this way, the L-arabinose induction process is no longer required.

Bacteriophages are among the greatest threats to industrial citramalate production in *E. coli* cell factories [25]. The commonly employed restriction-modification (R-M) system and CRISPR-Cas systems offer limited protection against a narrow spectrum of phages. Bacteriophage contamination often involves a mix of phages with diverse characteristics. Moreover, these strategies can inadvertently trigger cell death by restricting the host genome [25, 37, 38]. The Ssp defense system endows *E. coli* with broad-spectrum phage resistance, as well as genome and fermentation stability [25]. In this study, The Ssp defense system effectively shielded *E. coli* BW25113 from phage infection without imposing any notable metabolic burden on the host cell. As shown in Fig. 3A, the Ssp defense system had a slightly negative effect on the growth rate of the *E. coli* BW25113. In a previous study, the expression of the site-specific adenine methylase from an exogenous R-M system caused the *E. coli* K-12 strains to grow slowly by inducing the SOS DNA repair response [39]. The Ssp defense system, made up of the *sspBCDE* gene cassette, is a DNA phosphorothioation (PT)-based defense module in *E. coli* 3234/A with functions analogous to those of DNA methylation-based R-M systems. Similarly, the PT modification may also lead to comparable physiological changes in *E. coli* BW25113, resulting in slower growth of strain BW2 compared with the wild-type strain. The citramalate biosynthesis ability of strain CM8 was unaffected by the presence of T4 phage (Fig. 3B). These findings align with those reported by Zou et al. (2022), and the engineered *E. coli* MG1655 phage-resistant strains maintained their ability to produce recombinant proteins in the presence of phages [25].

Compared to the wild-type *MjCimA*, *MjCimA3.7*, with enhanced affinity and catalytic efficiency for acetyl-CoA, can significantly improve citramalate production (Fig. 4A), indicating that the acetyl-CoA supply may be a bottleneck for citramalate biosynthesis in *E. coli* [11]. This is consistent with previous report that citramalate production by *E. coli* has a linear relationship with the intracellular acetyl-CoA concentration [10]. Citramalate production in *E. coli* was significantly increased by weakening or deleting citrate synthase, which catalyzes citrate

synthesis from acetyl-CoA. However, the mutant strain lacking functional citrate synthase cannot solely grow on glucose and necessitates the presence of additional glutamate for growth [10, 11]. While the pyruvate dehydrogenase complex E2 subunit overexpression enhances the supply of acetyl-CoA, carbon loss takes place during decarboxylation, resulting in a notable reduction in the anticipated yield of products originating from acetyl-CoA [40]. The NOG pathway avoids CO<sub>2</sub> emissions during the acetyl-CoA yield was introduced to *E. coli* BW3 strain. Given that the NOG pathway competes with the Embden-Meyerhof-Parnas and pentose phosphate pathways for precursors, precise control of metabolic flux within this pathway is essential. *Bafxpk* expressing was under the control of the P<sub>J23102</sub> promoter with an appropriate transcriptional strength that did not affect the growth of the strain [30]. Strain CM11 exhibited significant improvements compared to CM8 in citramalate production, yield on glucose, and specific production, showing increases of 35.0%, 33.3%, and 12.2%, respectively (Fig. 4A and B). These enhancements were attributed to a greater supply of acetyl-CoA (Fig. 4C). This trend aligns with findings from a previous study on L-leucine synthesis, where utilization of pyruvate and acetyl-CoA led to similar outcomes. The strain employing the NOG pathway demonstrated a 28.1% increase in L-leucine production and a 28.6% increase in yield [30].

Elevated levels of intracellular acetyl-CoA can lead to NADH accumulation, potentially inhibiting glyceraldehyde phosphate dehydrogenase and, consequently, impacting glucose uptake [11]. Strain CM11 exhibited a reduced rate of glucose consumption compared to CM10. In *E. coli*, glucose uptake and phosphorylation are facilitated by the PTS system, a crucial component of the intricate regulatory mechanisms developed by bacteria to coordinate metabolism through complex signal transduction cascades [33]. Therefore, PTS is a frequently used target in metabolic engineering interventions [41]. The glucose facilitator protein *ZmGlf* has been used together with glucokinase from *E. coli* to improve glucose utilization in *E. coli* with inactivated PTS to improve the supply of acetyl-CoA [32]. In this study, the resulting strain CM12, showed a higher glucose utilization rate and citramalate production than those of CM11, suggesting that the manipulation of glucose consumption increased citramalate production. A comparable observation was noted in previous studies, wherein glucose utilization and succinate production were enhanced in PTS<sup>-</sup> strains through the recruitment of *ZmGlf* and *EcGlc* [32]. Although the citramalate yield on glucose decreased, this was likely a consequence of heightened glucose consumption. This increased consumption can be attributed to the non-PTS system. In this process, PEP is not consumed to produce pyruvate, a precursor for citramalate

biosynthesis, through the PTS system. Thus, the supply of pyruvate depends on glycolysis [42]. Moreover, the processes of carbon source utilization and product synthesis in *E. coli* are controlled by complex regulatory networks, including multiple enzymatic catalyzes and transcriptional regulation processes [21].

During fed-batch cultivation, the generated phage-resistant CM12 strain produced citramalate at a titer of 110.2 g/L in 80 h without the need to add expensive yeast extract or an additional induction process in fed-bath fermentation, which is the highest production and productivity reported to date (Table 3). A delay in citramalate production occurred, which may also be related to a change in the carbon source utilization pattern [21]. Future studies that focus on understanding the effect of metabolic engineering on metabolic flux distribution and further engineering modifications are needed to overcome this problem. In addition, the citramalate yield on glucose of strain CM12 was 0.4 g/g glucose during the fed-batch process, whereas engineered *E. coli* resulted in a yield of 0.5 g/g and 0.8 g/g glucose, respectively, in previous studies [12]. In the latter studies, fed-bath fermentation medium were supplemented with significant amounts of glutamate, leucine, yeast extract, or peptone. These substances can be assimilated by the cell, which in turn makes more glucose available for citramalate synthesis [2, 11].

This study demonstrates that optimizing *cimA* expression, augmenting acetyl-CoA supply, and carbon utilization represent effective strategies for elevating citramalate production in phage-resistant *E. coli*, offering promising prospects for industrial implementation. Moreover, the methodologies devised herein hold the potential to enhance the production of various other high-value compounds.

## Conclusion

In this study, a phage-resistant microbial cell factory for citramalate production from glucose was constructed by engineering an *E. coli* strain. By overexpressing *MjcimA3.7* and establishing a phage-resistant system in *E. coli* BW25113, a citramalate-producing strain with phage-resistant capability was constructed. Additionally, the citramalate titer was improved by introducing the NOG pathway and eliminating the synthesis of acetate byproducts to improve acetyl-CoA availability. Furthermore, the citramalate titer was improved by replacing native *ptsG* and *galR* with *Ecglk* and *Zmglf*, respectively, to improve the glucose utilization capacity of *E. coli*. Finally, the best strain achieved a citramalate titer of 110.2 g/L with a yield and productivity of 0.4 g/g glucose and 1.4 g/(L·h), respectively, during fed-batch fermentation without the need for expensive yeast extract or additional inducers. To the best of our knowledge, this is the

highest citramalate titer and productivity obtained using a less expensive substrate. Thus, the proposed approach appears to be viable for the efficient industrial-scale biosynthesis of citramalate and its derivatives.

#### Abbreviations

MMA	methyl methacrylate
PMMA	poly(methyl methacrylate)
MAA	methacrylic acid
TCA	tricarboxylic acid cycle
PCR	polymerase chain reaction
CRISPR	clustered regularly interspaced short palindromic repeat
CimA	citramalate synthase
NOG pathway	Non-oxidative glycolysis pathway
PEP	phosphoenolpyruvate

#### Supplementary Information

The online version contains supplementary material available at <https://doi.org/10.1186/s12934-024-02505-y>.

Supplementary Material 1

#### Author contributions

TW and LD conducted the experiments and wrote the manuscript. HL, HH, XS, YB, TT, YW (Yuan Wang), XQ, HZ, YW (Yaru Wang), and BY designed and supervised the work. JZ and XW conceived the research and reviewed the manuscript.

#### Funding

This research was supported by the National Key R&D Program of China (2021YFD1301001), the Agricultural Science and Technology Innovation Program (CAAS-ZDRW202304), and the China Agriculture Research System of MOF and MARA (CARS-41).

#### Data availability

No datasets were generated or analysed during the current study.

#### Declarations

##### Ethics approval and consent to participate

This article does not contain any studies with human participants or animal performed by any of the authors.

##### Consent for publication

All authors have read and approved this manuscript to publish.

##### Competing interests

The authors declare no competing interests.

Received: 3 June 2024 / Accepted: 8 August 2024

Published online: 22 August 2024

#### References

- Jee SH, Friedman E, Etzel RA, Nguyen VT, Sack TL, Kemper KJ. Climate change imperils pediatric health: child advocacy through fossil fuel divestment. *Yale J Biol Med*. 2023;96(2):233–9.
- Parimi NS, Durie IA, Wu X, Niyas AMM, Eiteman MA. Eliminating acetate formation improves citramalate production by metabolically engineered *Escherichia coli*. *Microb Cell Fact*. 2017;16(1):114.
- Lebeau J, Efronson JP, Lynch MD. A review of the biotechnological production of methacrylic acid. *Front Bioeng Biotechnol*. 2020;8:207.
- Lee HK, Woo S, Baek D, Min M, Jung GY, Lim HG. Direct and robust citramalate production from brown macroalgae using fast-growing *Vibrio* sp. dhg. *Bioreour Technol*. 2024;394:130304.
- Arya AS, Lee SA, Eiteman MA. Differential sensitivities of the growth of *Escherichia coli* to acrylate under aerobic and anaerobic conditions and its effect on product formation. *Biotechnol Lett*. 2013;35(11):1839–43.
- Wu X, Tovilla-Coutiño DB, Eiteman MA. Engineered citrate synthase improves citramalic acid generation in *Escherichia coli*. *Biotechnol Bioeng*. 2020;117(9):2781–90.
- Wu ZY, Sun W, Shen Y, Pratas J, Suthers PF, Hsieh PH, Dwaraknath S, Rabinowitz JD, Maranas CD, Shao Z, Yoshikuni Y. Metabolic engineering of low-pH-tolerant non-model yeast, *Issatchenkia orientalis*, for production of citramalate. *Metab Eng Commun*. 2023;16:e00220.
- Chi H, Wang X, Shao Y, Qin Y, Deng Z, Wang L, Chen S. Engineering and modification of microbial chassis for systems and synthetic biology. *Synth Syst Biotechnol*. 2019;4(1):25–33.
- Chen A, Xie Y, Xie S, Liu Y, Liu M, Shi J, Sun J. Production of citramalate in *Escherichia coli* by mediating colonic acid metabolism and fermentation optimization. *Process Biochem*. 2022;121:1–9.
- Wu X, Eiteman MA. Synthesis of citramalic acid from glycerol by metabolically engineered *Escherichia coli*. *J Ind Microbiol Biotechnol*. 2017;44(10):1483–90.
- Wu X, Eiteman MA. Production of citramalate by metabolically engineered *Escherichia coli*. *Biotechnol Bioeng*. 2016;113(12):2670–75.
- Webb JP, Arnold SA, Baxter S, Hall SJ, Eastham G, Stephens G. Efficient bio-production of citramalate using an engineered *Escherichia coli* strain. *Microbiol (Reading)*. 2018;164(2):133–41.
- Los M. Minimization and prevention of phage infections in bioprocesses. *Methods Mol Biol*. 2012;834:305–15.
- Yang X, Yuan Q, Zheng Y, Ma H, Chen T, Zhao X. An engineered non-oxidative glycolysis pathway for acetone production in *Escherichia coli*. *Biotechnol Lett*. 2016;38(8):1359–65.
- Bogorad IW, Lin TS, Liao JC. Synthetic non-oxidative glycolysis enables complete carbon conservation. *Nature*. 2013;502(7473):693–7.
- Jatain I, Yadav K, Nitharwal RG, Arora D, Dubey KK. A system biology approach for engineering non-oxidative glycolysis pathway in *Streptomyces toxytricini* for high lipstatin biosynthesis. *Bioresour Technol Rep*. 2022;19:101188.
- Miyoshi K, Kawai R, Niide T, Toya Y, Shimizu H. Functional evaluation of non-oxidative glycolysis in *Escherichia coli* in the stationary phase under microaerobic conditions. *J Biosci Bioeng*. 2023;135(4):291–7.
- Zhao D, Yuan S, Xiong B, Sun H, Ye L, Li J, Zhang X, Bi C. Development of a fast and easy method for *Escherichia coli* genome editing with CRISPR/Cas9. *Microb Cell Fact*. 2016;15(1):205.
- Sharan SK, Thomason LC, Kuznetsov SG, Court DL. Recombineering: a homologous recombination-based method of genetic engineering. *Nat Protoc*. 2009;4(2):206–23.
- Chang F, Wang Y, Zhang J, Tu T, Luo H, Huang H, Bai Y, Qin X, Wang Y, Yao B, et al. Efficient production of  $\gamma$ -aminobutyric acid using engineered *Escherichia coli* whole-cell catalyst. *Enzyme Microb Technol*. 2024;174:110379.
- Wang Y, Xu J, Jin Z, Xia X, Zhang W. Improvement of acetyl-CoA supply and glucose utilization increases l-leucine production in *Corynebacterium glutamicum*. *Biotechnol J*. 2022;17(8):e2100349.
- Glazyrina J, Materne EM, Dreher T, Storm D, Junne S, Adams T, Greller G, Neubauer P. High cell density cultivation and recombinant protein production with *Escherichia coli* in a rocking-motion-type bioreactor. *Microb Cell Fact*. 2010;9:42.
- Atsumi S, Liao JC. Directed evolution of *Methanococcus jannaschii* citramalate synthase for biosynthesis of 1-propanol and 1-butanol by *Escherichia coli*. *Appl Environ Microbiol*. 2008;74(24):7802–8.
- You R, Wang L, Shi C, Chen H, Zhang S, Hu M, Tao Y. Efficient production of myo-inositol in *Escherichia coli* through metabolic engineering. *Microb Cell Fact*. 2020;19(1):109.
- Zou X, Xiao X, Mo Z, Ge Y, Jiang X, Huang R, Li M, Deng Z, Chen S, Wang L, Lee SY. Systematic strategies for developing phage resistant *Escherichia coli* strains. *Nat Commun*. 2022;13(1):4491.
- Bassalo MC, Garst AD, Halweg-Edwards AL, Grau WC, Domaille DW, Mutalik VK, Arkin AP, Gill RT. Rapid and efficient one-step metabolic pathway integration in *E. coli*. *ACS Synth Biol*. 2016;5(7):561–8.
- Eriksen RS, Larsen F, Svenningsen SL, Sneppen K, Mitarai N. The dynamics of phage predation on a microcolony. *Biophys J*. 2024;123(2):147–56.
- Zhang Y, He Y, Zhang N, Gan J, Zhang S, Dong Z. Combining protein and metabolic engineering strategies for biosynthesis of melatonin in *Escherichia coli*. *Microb Cell Fact*. 2021;20(1):170.
- Zhou L, Wang Q, Shen J, Li Y, Zhang H, Zhang X, Yang S, Jiang Z, Wang M, Li J et al. Metabolic engineering of glycolysis in *Escherichia coli* for efficient

- production of patchoulol and  $\tau$ -cadinol. *Bioresour Technol.* 2024; 391(Pt B): 130004.
30. Ding X, Yang W, Du X, Chen N, Xu Q, Wei M, Zhang C. High-level and -yield production of L-leucine in engineered *Escherichia coli* by multistep metabolic engineering. *Metab Eng.* 2023;78:128–36.
  31. Lin PP, Jaeger AJ, Wu TY, Xu SC, Lee AS, Gao F, Chen PW, Liao JC. Construction and evolution of an *Escherichia coli* strain relying on nonoxidative glycolysis for sugar catabolism. *Proc Natl Acad Sci U S A.* 2018;115(14):3538–46.
  32. Zhang S, Yang W, Chen H, Liu B, Lin B, Tao Y. Metabolic engineering for efficient supply of acetyl-CoA from different carbon sources in *Escherichia coli*. *Microb Cell Fact.* 2019;18(1):130.
  33. Meadow ND, Savtchenko RS, Nezami A, Roseman S. Transient state kinetics of enzyme IICB<sup>glc</sup>, a glucose transporter of the phosphoenolpyruvate phosphotransferase system of *Escherichia coli*: equilibrium and second order rate constants for the glucose binding and phosphotransfer reactions. *J Biol Chem.* 2005;280(51):41872–80.
  34. Niu D, Tian K, Prior BA, Wang M, Wang Z, Lu F, Singh S. Highly efficient L-lactate production using engineered *Escherichia coli* with dissimilar temperature optima for L-lactate formation and cell growth. *Microb Cell Fact.* 2014;13:78.
  35. Valgepea K, Adamberg K, Nahku R, Lahtvee PJ, Arike L, Vilu R. Systems biology approach reveals that overflow metabolism of acetate in *Escherichia coli* is triggered by carbon catabolite repression of acetyl-CoA synthetase. *BMC Syst Biol.* 2010;4:166.
  36. Xiong B, Li Z, Liu L, Zhao D, Zhang X, Bi C. Genome editing of *Ralstonia eutropha* using an electroporation-based CRISPR-Cas9 technique. *Biotechnol Biofuels.* 2018;11:172.
  37. Liu L, Zhao D, Ye L, Zhan T, Xiong B, Hu M, Bi C, Zhang X. A programmable CRISPR/Cas9-based phage defense system for *Escherichia coli* BL21(DE3). *Microb Cell Fact.* 2020;19(1):136.
  38. Mruk I, Kobayashi I. To be or not to be: regulation of restriction-modification systems and other toxin-antitoxin systems. *Nucleic Acids Res.* 2014;42(1):70–86.
  39. Heitman J, Model P. Site-specific methylases induce the SOS DNA repair response in *Escherichia coli*. *J Bacteriol.* 1987;169(7):3243–50.
  40. Wang Q, Xu J, Sun Z, Luan Y, Li Y, Wang J, Liang Q, Qi Q. Engineering an in vivo EP-bifido pathway in *Escherichia coli* for high-yield acetyl-CoA generation with low CO<sub>2</sub> emission. *Metab Eng.* 2019;51:79–87.
  41. Sánchez-Cañizares C, Prell J, Pini F, Rutten P, Kraxner K, Wynands B, Karunakaran R, Poole PS. Global control of bacterial nitrogen and carbon metabolism by a PTS<sup>Ntr</sup>-regulated switch. *Proc Natl Acad Sci U S A.* 2020;117(19):10234–45.
  42. Alva A, Sabido-Ramos A, Escalante A, Bolívar F. New insights into transport capability of sugars and its impact on growth from novel mutants of *Escherichia coli*. *Appl Microbiol Biotechnol.* 2020;104(4):1463–79.

### Publisher's Note

Springer Nature remains neutral with regard to jurisdictional claims in published maps and institutional affiliations.